THE JOURNAL OF BIOLOGICAL CHEMISTRY
Vol. 276, No. 18, Issue of May 4, pp. 15511–15518, 2001
Printed in U.S.A.

Interactions of the Cold Shock Protein CspB from *Bacillus subtilis* with Single-stranded DNA

IMPORTANCE OF THE T BASE CONTENT AND POSITION WITHIN THE TEMPLATE*

Received for publication, November 20, 2000, and in revised form, January 24, 2001
Published, JBC Papers in Press, January 29, 2001, DOI 10.1074/jbc.M010474200

Maria M. Lopez‡, Katsuhide Yutani§, and George I. Makhatadze‡¶

From the ‡Department of Biochemistry and Molecular Biology, Penn State University, College of Medicine, Hershey, Pennsylvania 17033 and the §Institute for Protein Research, Osaka University, 3-2 Yamadaoka, Suita, Osaka 565-0871, Japan

The cold shock protein CspB from *Bacillus subtilis* binds T-based single-stranded DNA (ssDNA) with high affinity (Lopez, M. M., Yutani, K., and Makhatadze, G. I. (1999) *J. Biol. Chem.* 274, 33601–33608). In this paper we report the results of CspB interactions with non-homogeneous ssDNA templates containing continuous and non-continuous stretches of T bases. The analysis of CspB-ssDNA interactions was performed using fluorescence spectroscopy, analytical centrifugation and isothermal titration calorimetry. We show that (i) there is a strong correlation between the CspB affinity and stoichiometry and the T content in the oligonucleotide that is independent of which other bases are incorporated into the sequence of ssDNA; (ii) the binding properties of CspB to ssDNA templates with continuous or non-continuous stretches of T bases with similar T content is very similar, and (iii) the mechanism of interaction between CspB and the T-based non-homogeneous ssDNA is mainly through the bases (a stretch of three T bases located in the middle of the ssDNA templates makes the binding independent of the ionic strength). The biological relevance of these results to the role of CspB as an RNA chaperone is discussed.

The detailed mechanism by which living cells survive a cold shock remains controversial (1). It has been observed that in many bacteria cold shock is accompanied by an increase in the expression levels of a specific set of the so-called cold shock proteins (CSPs)[1] (2, 3). In *Bacillus subtilis* the major CSP is a small acidic protein, CspB, whose induction increases dramatically when the temperature is down-shifted from 37°C to 15 °C (4). The first evidence of any activity of CspB was demonstrated using gel retardation experiments, and it was shown that CspB binds to single-stranded DNA (ssDNA) containing the Y-box motif (ATTGG) (5, 6). Later, however, it was shown that CspB binding is not limited only to this sequence (7, 8). Several aromatic residues (Phe^{15}, Phe^{17}, Phe^{27}, Phe^{30}, Phe^{38}, Trp^{8}) and several basic amino acid residues (His29, Lys^{7}, Lys^{13}, Lys^{39}, Arg^{56}) have been proposed to be involved in the protein interaction with ssDNA (9). The three-dimensional structure of the protein shows that these amino acid residues are located in the same side of the protein molecule (5, 6).

In our laboratory, using four different techniques (gel shift mobility assays, isothermal titration calorimetry (ITC), analytical ultracentrifugation, and fluorescence spectroscopy), it was shown that CspB binds preferentially to polypyrimidine ssDNA (8). CspB binding to poly(dC) and poly(dT) has different properties showing higher affinity for homogeneous T-based oligonucleotides with a binding site size of 6–7 T bases (8). The analysis of such binding according to the Epstein model (10) showed that the CspB binding to T-based ssDNA template has high affinity ($K_a \sim 3 \times 10^6$ M^{-1}) and moderate cooperativity ($\omega \sim 16$). To further characterize the CspB binding to T-based ssDNA templates, two major questions must be answered. 1) How is CspB binding to continuous stretches of T bases affected by the presence of other bases in the oligonucleotide? 2) How is such a binding affected when the T bases form non-continuous stretches? To address these questions, we used fluorescence spectroscopy, analytical centrifugation, and isothermal titration calorimetry and measured the CspB binding properties to series of ssDNA (23-mers) in which the T bases were placed in the middle of the oligonucleotide (23CpTi, 23ApTi, and 23GpTi, where i = 3, 5, 7, 11, 15, and 17), forming a continuous stretch but varying its length. The results of these experiments were compared with the effect of non-continuous stretches of T bases, the effect of location of the T bases within short ssDNA template and the effect of the total length of the oligonucleotide on the CspB binding. In addition, the nature of the mechanism responsible for the CspB binding to non-homogeneous ssDNA template was investigated by comparing the binding profiles at high (1 M) and low (0.1 M) NaCl concentrations.

Our results show that ssDNA binding properties of CspB are strongly correlated with the T-base content in the ssDNA templates. Indeed, ssDNA templates with similar T content have similar binding properties, independent of whether the T bases form continuous or non-continuous stretches. We also show that the forces involved in the CspB binding to most of the non-homogeneous T-based ssDNA template are not via electrostatic interactions of protein groups with the phosphate backbone because no difference in the binding profiles is observed under experimental conditions with different ionic strength. This implies that the interactions of CspB with non-homogeneous T-based ssDNA templates occur mainly through the bases. These observations combined with the sequence analysis of 5′-UTR of cold shock-inducible proteins suggests possible function of CspB as RNA chaperone.

* This work was supported by Human Frontier in Science Program Grant RPG-0036/1997M. The costs of publication of this article were defrayed in part by the payment of page charges. This article must therefore be hereby marked "*advertisement*" in accordance with 18 U.S.C. Section 1734 solely to indicate this fact.

¶ To whom correspondence should be addressed: Dept. of Biochemistry and Molecular Biology, Penn State University College of Medicine, Hershey, PA 17033. Tel.: 717-531-0712; Fax: 717-531-7072; E-mail: makhatadze@psu.edu.

[1] The abbreviations used are: CSP, cold shock protein; UTR, untranslated region; ssDNA, single-stranded DNA; ITC, isothermal titration calorimetry.

MATERIALS AND METHODS

CspB and ssDNA Purification—CspB was overexpressed in *Escherichia coli* and purified as described previously (8, 11). The protein concentration was measured spectrophotometrically using the extinction coefficient ϵ_{280} = 5,690 M^{-1} cm^{-1} (8). The ssDNA oligonucleotides were obtained from Biosynthesis Inc. and purified as described previously (8). The ssDNA concentration was calculated considering the following extinction coefficients at 260 nm: 8400 M^{-1} cm^{-1} (for T), 12010 M^{-1} cm^{-1} (for G), 7050 M^{-1} cm^{-1} (for C), and 15,200 M^{-1} cm^{-1} (for A) (12).

Analytical Centrifugation Experiments—The analytical centrifugation experiments were performed in a Beckman XLA ultracentrifuge. The runs were performed at 4 °C under two different speeds, 20,000 and 25,000 rpm, until equilibrium was achieved (usually >10 h). Absorbencies at 260 and 280 nm were recorded simultaneously for three cells. Each cell contained only ssDNA, CspB, or CspB-ssDNA complex. The ssDNA concentrations were 2 μM for 23ApT3 and 23ApT11 and 2.5 μM for 23CpT3, 23CpT7, and 23CpT11. The protein concentration was 20-fold higher than the ssDNA concentration. The CspB-ssDNA complex concentration was the same as in the other cells. To allow for the complex formation, the protein was incubated with the ssDNA at room temperature for 25 min prior to each run. The partial specific volume for the protein, ssDNA, and complex were 0.74, 0.55, and 0.65 cm^3/g, respectively and calculated as described previously (8).

ITC—ITC experiments were performed using a VP-ITC (Microcal Inc. Northampton, MA) instrument. The protein and ssDNA were dialyzed simultaneously in 50 mM Tris, pH 7.5, 100 mM NaCl buffer. The protein concentration was usually between 10 and 15 μM. Typical concentrations of the ssDNA were between 85 and 135 μM. Series of several injections of 5 or 10 μl each of solution containing ssDNA template into ITC cells containing CspB were made until no further heat effect was observed. The heat of dilution was measured by injecting identical amounts of ssDNA into the ITC cell containing only buffer. The heat of the reaction was obtained by integration of the peak area after each injection of ssDNA solution, using ORIGIN software provided by the manufacturer. ΔH_{cal} was calculated by summing the individual heats, corrected for the heats of dilution, and dividing by the total number of moles of CspB present in the ITC cell during the experiment. Detailed description of the ITC experiment has been reported previously (8).

Fluorescence Measurements—The CspB fluorescence intensity was measured using a FluoroMax spectrofluorometer with DM3000F software and thermostated cell holder connected to a circulating water bath. The equilibrium titrations were performed at low (0.3 μM) protein concentration in 50 mM Tris-HCl, pH 7.5, with 100 mM NaCl (low ionic strength) or 1 M NaCl (high ionic strength). Tryptophan fluorescence was excited at 287 nm, and the emission was recorded at 349 nm. Stoichiometric titrations were performed at high protein concentration (14 μM) in low ionic strength buffer. The excitation and emission wavelengths were 300 and 349 nm, respectively. All experiments were performed at 25 °C, and the initial volume in the sealed quartz cell was 1.1 ml. Small aliquots of concentrated solutions of ssDNA were added into the cell containing solution of CspB. The solution in the cell was gently stirred during the titration and the intensity values were corrected by dilution; inner filter effect and blanks were subtracted.

The equilibrium titration profiles, under conditions when only one molecule of CspB was bound to the ssDNA template, were fitted to Equation 1 (8).

$$Q = Q_{max} \frac{([CspB]_{tot} + [ssDNA]_{tot} + 1/K_a) - \sqrt{([CspB]_{tot} + [ssDNA]_{tot} + 1/K_a)^2 - 4[CspB]_{tot}[ssDNA]_{tot}}}{2[CspB]_{tot}} \quad \text{(Eq. 1)}$$

Q represents the quenching effect on the CspB Trp fluorescence after each addition of ssDNA, Q_{max} is the maximal quenching obtained upon complete saturation of the protein with ssDNA, $[CspB]_{tot}$ and $[ssDNA]_{tot}$ are the total concentration of protein and ssDNA in solution, respectively, and K_a is the equilibrium association constant for the CspB-ssDNA interaction.

RESULTS

Previously, using a combination of four different techniques, we showed that CspB seems to bind T-containing homogeneous ssDNA template with much higher affinity (K_d = 42 nM at 25 °C) than C-, G-, or A-containing 23-mer homogeneous ssDNA templates (13). In this study we used hetero-ssDNA templates to investigate how the change in length of a T stretch flanked by other nucleotides (A, C, and G), the relative position of the T stretches within the template and continuous *versus* non-continuous stretches of T bases affect the thermodynamics of the CspB-ssDNA interactions. With few exceptions the ssDNA templates were 23 nucleotides long (Table I). CspB-ssDNA interactions were monitored using three different techniques: fluorescence spectroscopy, isothermal titration calorimetry, and analytical centrifugation.

Effect of 23-mer Non-homogeneous ssDNA Templates with Different Number of T Bases on the CspB Tryptophan Fluorescence—The changes in the protein intrinsic tryptophan fluorescence is a widely used to monitor protein-DNA interactions (*e.g.* Refs. 14 and 15). The cold shock protein CspB has only one Trp residue that is located in the putative nucleic acid binding face of the protein (9). The fluorescence intensity of this Trp is dramatically quenched upon interaction with T-based ssDNA templates (8). This quenching of CspB Trp fluorescence correlates with the degree of binding upon the CspB-ssDNA interactions (8).

Fig. 1 (*A–C*) shows the quenching effects caused by non-homogeneous ssDNA templates 23CpTi, 23GpTi, and 23ApTi (i = 3, 5, 7, 11, 15, and 17; see Table I for sequences) on the CspB intrinsic Trp fluorescence. In all cases there is a shift in the titration profiles toward lower ssDNA concentrations as the number of T bases in ssDNA template increases. The difference in the binding competences, defined as $[ssDNA]_{0.5}$, between *X*T3 and *X*T17, where *X* represents C, G, or A bases, is about 1 order of magnitude (from $\sim 4 \times 10^{-7}$ M to $\sim 6 \times 10^{-8}$ M, respectively). Comparing the three series of ssDNA templates (23CpTi, 23GpTi, and 23ApTi), it is clear that ssDNA templates with the same T content behave in very similar fashion in the 23CpTi and 23GpTi series (Fig. 1, *A* and *B*). In fact, there is a good correspondence between the binding competences for the ssDNA templates with the same number of T bases in both series (Fig. 2). The correlation coefficient is 0.98, indicating that the interaction is independent of the presence of C or G bases surrounding the stretches of T. This result strongly indicates that the CspB interactions with these ssDNA templates are probably independent of three-dimensional structure of ssDNA in agreement with previous results (13).

The titration profiles of CspB with the 23ApTi template series are different than the ones obtained with the 23CpTi or 23GpTi series (Fig. 1, compare *C* with *A* and *B*). The titration profiles for the ssDNA templates 23ApT3, 23ApT5, 23ApT7, and 23ApT11 overlap. This result can be explained considering that, in the 23ApTi series, some of the ssDNA templates have the ability to form double-stranded DNA due to the classical Watson-Crick base pairing, as will be further supported by the analytical centrifugation data (see below). However, ssDNA templates with larger number of T bases (23ApT15 and 23ApT17) do show an enhancement in binding, as seen by the decrease in the $[ssDNA]_{0.5}$ as the stretch of T bases becomes longer (Fig. 1*C*).

Taken together, these results indicate that there is a strong correlation between the $[ssDNA]_{0.5}$ and the T content in the template when the T bases are located in the middle of the ssDNA template and form a continuous stretch. Observed differences in $[ssDNA]_{0.5}$ for different templates can arise from the changes in the affinity of binding and/or in the stoichiometry of the interaction.

It must be noted that the ssDNA templates used in this study are not homogeneous and relatively short (most of them are 23-mer). Unfortunately, no rigorous mathematical model has been developed for the analysis of the titration profiles in which more than one molecule of protein binds to the short and heterogeneous matrix (14, 16). To the best of our knowledge,

TABLE I
Sequence of the oligonucleotides used throughout this study

Name	Sequence	Length	No. of T	Salt effect[a]
23pT	5′–TTTTTTTTTTTTTTTTTTTTTTT	23	23	–
23pC	5′–CCCCCCCCCCCCCCCCCCCCCCC	23	0	+++
23CpT1	5′–CCCCCCCCCCCCTCCCCCCCCCC	23	1	++
23CpT2	5′–CCCCCCCCCCCCTTCCCCCCCCC	23	2	+
23CpT3	5′–CCCCCCCCCCCTTTCCCCCCCCC	23	3	–
23CpT5	5′–CCCCCCCCCTTTTTCCCCCCCCC	23	5	–
23CpT7	5′–CCCCCCCCTTTTTTTCCCCCCCC	23	7	–
23CpT11	5′–CCCCCCTTTTTTTTTTTCCCCCC	23	11	–
23CpT15	5′–CCCCTTTTTTTTTTTTTTTCCCC	23	15	–
23CpT17	5′–CCCTTTTTTTTTTTTTTTTTCCC	23	17	–
23GpT5	5′–GGGGGGGGGTTTTTGGGGGGGGG	23	5	ND
23GpT7	5′–GGGGGGGGTTTTTTTGGGGGGGG	23	7	ND
23GpT11	5′–GGGGGGTTTTTTTTTTTTGGGGGG	23	11	ND
23GpT15	5′–GGGGTTTTTTTTTTTTTTTGGGG	23	15	ND
23GpT17	5′–GGGTTTTTTTTTTTTTTTTTGGG	23	17	ND
23ApT3	5′–AAAAAAAAAATTTAAAAAAAAAA	23	3	ND*
23ApT5	5′–AAAAAAAAATTTTTAAAAAAAAA	23	5	ND*
23ApT7	5′–AAAAAAAATTTTTTTAAAAAAAA	23	7	ND*
23ApT11	5′–AAAAAATTTTTTTTTTTAAAAAA	23	11	ND*
23ApT15	5′–AAAATTTTTTTTTTTTTTTAAAA	23	15	–
23ApT17	5′–AAATTTTTTTTTTTTTTTTTAAA	23	17	–
$23CT_2$	5′–CCCCCCCCCCATTGGCCCCCCCCC	23	2	++
$23CT_4$	5′–CCCCCCCCCTATTGGTCCCCCCCC	23	4	ND
$23CT_8$	5′–CCCCCCTTTATTGGTTTCCCCCC	23	8	–
$23CT_{12}$	5′–CCCCTTTTTATTGGTTTTTCCCC	23	12	ND
T5C7T5	5′–TTTTTCCCCCCCTTTTT	17	10	–
T7C7T7	5′–TTTTTTTCCCCCCCTTTTTTT	21	14	ND
T9C7T9	5′–TTTTTTTTTCCCCCCCTTTTTTTTT	25	18	ND
T14C7T14	5′–TTTTTTTTTTTTTTTCCCCCCCTTTTTTTTTTTTTT	35	28	ND
T18C7T18	5′–TTTTTTTTTTTTTTTTTTTCCCCCCCTTTTTTTTTTTTTTTTTT	43	36	ND
23pT6G	5′–TTTGGGGGGGGGGGGGGGGTTT	23	6	++
23pT8G	5′–TTTTGGGGGGGGGGGGGGTTTT	23	8	+
23pT12G	5′–TTTTTTGGGGGGGGGGGTTTTTT	23	12	–
23pT16G	5′–TTTTTTTTGGGGGGGTTTTTTTT	23	16	–
23pT18G	5′–TTTTTTTTTGGGGGTTTTTTTTT	23	18	–
23pT20G	5′–TTTTTTTTTTGGGTTTTTTTTTT	23	20	–

[a] The effect of 1 M NaCl on the titration profiles of CspB as monitored by fluorescence spectroscopy. +++, complete elimination of binding in high salt; ++, significant decrease of binding in high salt; +, detectable decrease of binding in high salt; –, no change of binding in high salt; ND, not determined; ND*, not determined because of the possible formation of dsDNA.

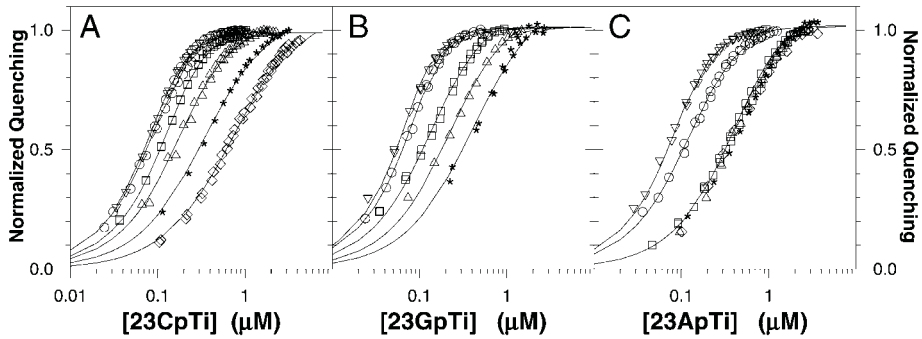

FIG. 1. **Normalized quenching effect of the CspB intrinsic tryptophan fluorescence intensity by ssDNA templates 23CpTi (*A*), 23GpTi (*B*), and 23ApTi (*C*).** The *symbols* represent *X*T3 (◇), *X*T5 (*), *X*T7 (△), *X*T11 (□), *X*T15 (○), and *X*T17 (▽), where *X* denotes C, G, or A bases. Titration with 23GT3 is not included (see "Materials and Methods"). The *line* through the experimental points has no meaning but to guide the eye, except for 23ApT3 and 23ApT11, which represent the fit of experimental data to Equation 1 (see "Materials and Methods"). The protein concentration was 0.3 μM in 50 mM Tris-HCl, pH 7.5, 100 mM NaCl. The excitation and emission wavelengths were 287 and 349 nm, respectively.

the mathematical models available to date have been developed either for homogeneous and infinitely long linear templates (17), or for homogeneous and short lattices (10) or even homogeneous templates for which linearity between the signal change and the fractional saturation does not necessarily hold during the binding reaction, but not for short non-homogeneous templates (for reviews, see Refs. 14 and 16). We thus are not able to estimate the CspB/ssDNA binding affinities. We can, however, experimentally estimate the stoichiometry of the CspB binding to non-homogeneous ssDNA templates using analytical centrifugation and isothermal titration calorimetry.

Stoichiometry of Non-homogeneous ssDNA-CspB Complexes—For homogeneous ssDNA templates, it was shown that three CspB molecules bind to 23pT and only one CspB molecule binds to 23pC (8). However, the templates used in present study are not homogeneous, and thus different stoichiometry among templates with different T-content is expected.

The stoichiometry for several of the 23CpTi-CspB and 23ApTi-CspB complexes was determined by analytical centrifugation. The apparent molecular masses of the ssDNA, CspB, and the ssDNA-CspB complex were measured simultaneously in the same experiment. The results are summarized in Table

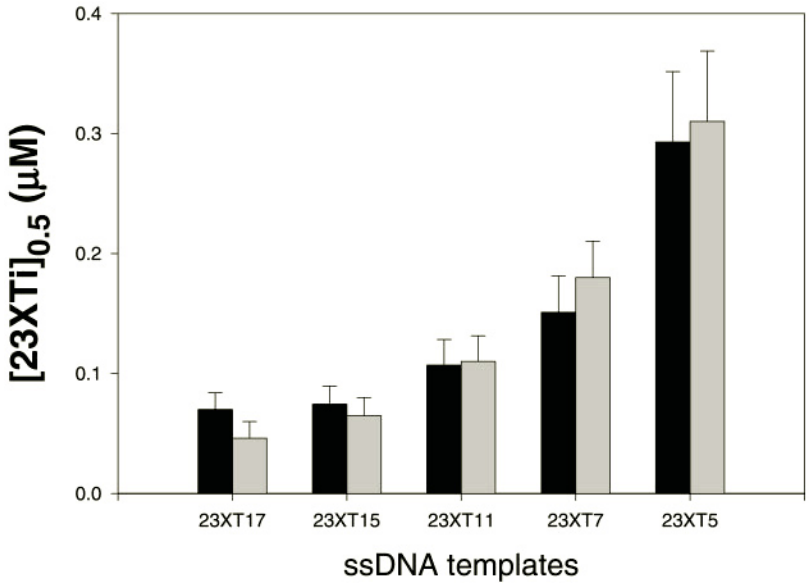

FIG. 2. **Comparison of the CspB binding competencies for 23CpTi (*black bars*) and 23GpTi (*gray bars*) series of ssDNA templates.**

II. Under our experimental conditions, the average molecular masses for the protein and the 23CpTi ssDNA (8.0 ± 0.4 and 7.1 ± 0.2 kDa, respectively) are in good correspondence with the expected values for monomeric species (7.5 and 6.9 kDa, respectively) (Fig. 3*A*). Considering the apparent molecular masses of the CspB:23CpTi complexes and individual species (Table II), we find that two molecules of CspB bind to 23CpT3, 23CpT7, and 23CpT11. Although this result is clear for the 23CpT7 and 23CpT11 templates, a lower value was obtained for 23CpT3 (the ratio CspB:23CpT3 is 1.5). Nevertheless, isothermal titration calorimetry experiments (see below) support our conclusion that more than one molecule of CspB binds to 23CpT3. We can therefore conclude that the difference in binding competences observed in the equilibrium titration profiles from 23CpT3 to 23CpT11 (Fig. 1*A*) is due to an increase in the protein effective binding affinity and not due to a change in the stoichiometry of the interaction. It is notable that the increase in effective binding affinity directly correlates with the T-content in the ssDNA.

The calculated stoichiometries for 23ApT3 and 23ApT11 show that these oligonucleotides bind only one CspB molecule (Table II). This is not surprising for 23ApT3 because CspB does not bind to homogeneous A-based templates (8). So, if one molecule of CspB binds to the three T bases in 23ApT3, this will represent an "imperfect" binding because we have shown previously using 23pT template that the CspB binding site size is 6–7 bases long (8). An imperfect binding should translate into a lower affinity of the protein for this ssDNA, as is observed experimentally (Fig. 1*C*). When only one molecule of protein binds to the ssDNA template, the interaction is accurately described by the classical binding equation (see Equation 1, under "Materials and Methods"), and it has been used to describe the thermodynamics of binding in different protein-DNA systems (8, 18). From the fit of the titration profile of CspB with ssDNA templates to Equation 1, the calculated equilibrium association constant (K_a) for CspB interaction with 23ApT3 is $(4.3 \pm 0.1) \times 10^6\ \text{M}^{-1}$, which is indeed lower than the effective affinity for 23pT $\sim 5 \times 10^7\ \text{M}^{-1}$ (8). In contrast, 23ApT11 has enough T bases to bind one molecule of CspB with the same affinity as 23pT. Experimentally, however, we observe that the normalized titration curve for 23ApT11 overlaps with that for 23ApT3 (Fig. 1*C*), indicating that 23ApT3 and 23AT11 have comparable affinities. The fit of the CspB:23ApT11 titration curve to Equation 1 gives an equilibrium constant K_a of $(4.4 \pm 0.1) \times 10^6\ \text{M}^{-1}$, identical to that of 23ApT3 but an order of magnitude lower than the effective affinity for 23pT. The reason why the CspB molecule bound to 23ApT11 presents lower affinity than expected seems to be related to the fact that this non-homogeneous template has the ability to form double-stranded DNA. Indeed, the measured molecular mass for the 23ApT11 template is higher than that predicted for the ssDNA (10.1 ± 0.1 kDa *versus* 6.8 kDa, respectively, Table II), indicating probably the presence of a significant population of double-stranded DNA under our experimental conditions. CspB does not have detectable affinity to double-stranded DNA (5, 6). Thus, if at least part of the 23ApT11 forms double-stranded DNA via classical Watson-Crick A-T base pairing, the effective concentration of ssDNA will be overestimated and that would result in a lower apparent affinity, as is observed experimentally (Fig. 1*C*).

TABLE II
Molecular masses obtained by analytical centrifugation for the ssDNA, ssDNA-CspB complex, and CspB

The experimental conditions are described under "Materials and Methods."

ssDNA	Mass of ssDNA	Mass of complex	Mass of CspB	Stoichiometry $N_{CpsB/ssDNA}$
	kDa	*kDa*	*kDa*	
23CpT3	6.9 ± 0.4	18.6 ± 0.6	8.0 ± 0.5	1.5 ± 0.3
23CpT7	7.3 ± 0.1	21.2 ± 0.4	8.0 ± 0.5	1.7 ± 0.3
23CpT11	7.1 ± 0.1	22.4 ± 0.5	8.0 ± 0.5	1.9 ± 0.3
23ApT3	6.2 ± 0.2	13.7 ± 0.8	8.0 ± 0.5	0.9 ± 0.3
23ApT11	10.1 ± 0.1	16.6 ± 0.3	8.0 ± 0.5	0.8 ± 0.3

The stoichiometry of the CspB interaction with some of the oligonucleotides within the 23CpTi series was also studied using ITC. The protein solution (in the calorimetric cell) was titrated with the ssDNA (in the syringe) until no heat effects were observed. Under experimental conditions with high protein concentration (11–15 μM CspB in solution), we observe that the titration profiles are very steep and rapidly level off (Fig. 3*B*), allowing determination of the stoichiometry of the interaction from the breaking point in the titration profile. The breaking point for the 23CpT15 template is ~ 0.3, indicating that 3 molecules of CspB bind to 23CpT15. The titrations with 23CpT11 and 23CpT5 are shifted toward lower stoichiometry. The breaking point for the titrations of these two templates is at a ratio ssDNA/CspB ~ 0.5, indicating that 2 molecules of CspB bind to 23CpT11 and 23CpT5 templates. Finally, the titration with 23CpT3 is not as sharp as the other ones; how-

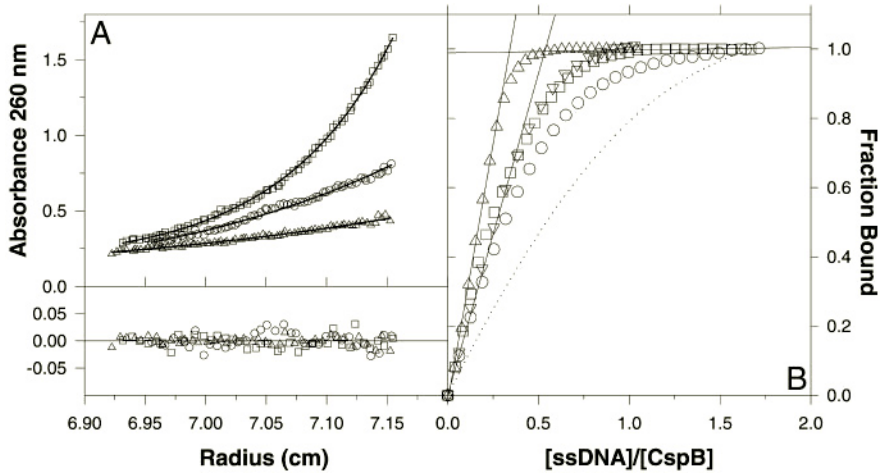

FIG. 3. **Interaction of CspB with ssDNA as monitored by analytical centrifugation (*A*) and isothermal titration calorimetry (*B*).** *Panel A* shows representative analytical centrifugation data obtained simultaneously for CspB (△), 23CpT11 (○), and the 23CpT11-CspB complex (□) at a protein:ssDNA ratio of 20:1. The *solid lines* represent the best fit of the data to the molecular masses 8.3, 7.1, and 22.4 kDa, respectively. Residuals of the fits shown are also included using the same *symbols* in both *graphs*. *Panel B* shows the changes in the fraction of CspB bound to 23CpT15 (△), 23CpT11 (□), 23CpT5 (▽), and 23CpT3 (○) as a function of the ssDNA:CspB ratio as determined by ITC. The *dotted line* represents the fit of the CspB titration with 23CpT3 considering one molecule of protein bound (see Equation 1 under "Materials and Methods"). The protein and ssDNA concentrations were 11–15 and 84–134 μM, respectively. The injections varied between 5 and 10 μl. The buffer conditions were same as defined in Fig. 1.

ever, the curve could not be fitted according to Equation 1 using 1:1 stoichiometry of CspB/ssDNA complex (Fig. 3*B*). This result suggests that more than one molecule of protein binds to the 23CpT3 template and supports our conclusion based on the analytical centrifugation experiments that probably two CspB molecules bind to 23CpT3 template. The enthalpies of the interaction per binding site for these oligonucleotides were -105 ± 9 kJ/mol, comparable to the values obtained for 23pT, -119 ± 6 kJ/mol (8). Similarity of the enthalpies of interactions with different T-based ssDNA templates suggests similar structural features for the CspB-ssDNA complexes.

In summary, the stoichiometries for the CspB interaction with the 23CpTi oligonucleotides determined by analytical centrifugation and ITC are in good agreement. The results show that 23CpT3, 23CpT5, 23CpT7, and 23CpT11 bind two CspB molecules. Knowing that the CspB binding site size is 6–7 T bases (8), our results suggest that not only the T bases but also the C bases are somehow involved in the CspB binding to those ssDNA templates. In addition, the ITC experiments show that there are changes in the total number of protein molecules bound to 23-mer ssDNA templates (two or three CspB molecules bind to 23-mer ssDNA templates depending on the number of T bases in the oligonucleotide).

Properties of the CspB Binding to 23-mer ssDNA with Non-continuous Stretch of T Bases—The experiments described in the previous sections have shown that CspB interactions with ssDNA templates vary with the number of T bases forming a continuous stretch (Table II, Figs. 1 (*A–C*) and 3*B*). To evaluate how the different content of T bases forming non-continuous stretches of T might affect the CspB-ssDNA interaction, the ATTGG sequence was incorporated in four 23-mer oligonucleotides: $23CT_2$, $23CT_4$, $23CT_8$, and $23CT_{12}$ (see Table I for sequence). The reason we chose this sequence to be incorporated into the ssDNA was that initially it was considered that CspB binds specifically to ATTGG sequence (19). Later, however, it has been shown that the CspB binding to ssDNA is not limited to this sequence (7, 8). Nevertheless, it constitutes a good model to study the CspB interaction with 23-mer ssDNA with non-continuous stretches of T bases. It is important to note that the T bases in these non-continuous stretches are only one or two bases apart. The normalized equilibrium titrations with these oligonucleotides are shown in Fig. 4. The binding curves for the

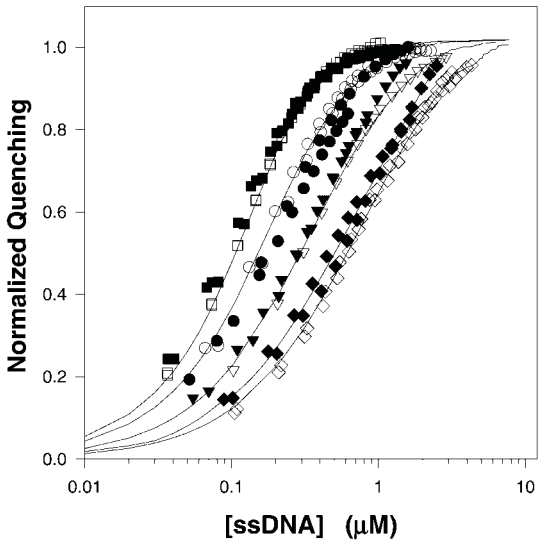

FIG. 4. **Normalized quenching effect of the CspB Trp fluorescence intensity by $23CT_{12}$ (■), $23CT_8$ (●), $23CT_4$ (▼), and $23CT_2$ (◆).** Titrations with 23CpT11 (□), 23CpT7 (○), 23CpT5 (▽), and 23CpT3 (◇) from Fig. 1 have been included for comparison. The *lines* through the experimental points have no meaning but to guide the eye.

CspB titration with $23CT_{12}$ (with a total of 12 T) and 23CpT11 (with a total 11 T) overlap. The same is observed for the CspB titrations with the other pairs of templates: $23CT_8$ (8 T bases) and 23CpT7 (7 T bases), $23CT_4$ (4 T bases), and 23CpT5 (5 T bases) and $23CT_2$ (2 T bases) and 23CpT3 (3 T bases). These results suggest that the $[ssDNA]_{0.5}$ for these oligonucleotides containing non-continuous stretches of T bases separated by one or two bases is very comparable to the values obtained for ssDNA with similar T content forming continuous stretches of T. The importance of the potential implications of these findings is obvious. First, it is not the local structure of the ssDNA that is important for CspB binding. Second, not all bases in the CspB binding site are equally important for the interaction. The latter is particularly significant because non-continuous stretches of T bases are more often found in DNA, as compared with long and continuous stretches of T bases.

CspB Binding to ssDNA Templates Containing Two Contin-

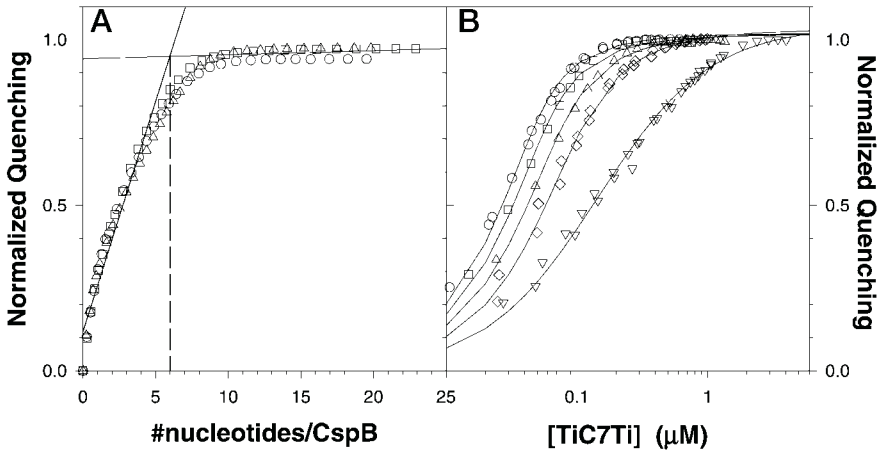

FIG. 5. **Stoichiometric (*panel A*) and equilibrium (*panel B*) titrations of CspB (14 and 0.3 μM, protein concentration, respectively) with T18C7T18 (○), T14C7T14 (□), T9C7T9 (▽), T7C7T7 (◇, not included in *panel A*), and T5C7T5 (▽, not included in *panel A*).**

uous Stretches of T Bases—The next step was to study the CspB binding to non-homogeneous oligonucleotides of different length with stretches of T in which the T bases were more than two bases apart and not in the middle of the template but situated at the ends. A constant stretch of seven C bases was always in the middle of these templates, which are flanked by different number of T bases (Table I). The reason C bases, as opposed to A or G, were selected to be in the middle of the oligonucleotides was to avoid possible double-stranded DNA formation (in the presence of A bases), and we chose seven because it appears that the size of the CspB binding site on T-based ssDNA template is 6–7 nucleotides long (8). Fig. 5*A* shows the titration profiles of CspB with T18C7T18, T14C7T14, and T9C7T9 under stoichiometric conditions. Since titrations were performed under stoichiometric conditions, we observe, from the breaking point in the titrations, that about 6 nucleotides are covered by a molecule of CspB in agreement with our previous observations (8). These results indicate that, when the T content in the ssDNA template is high (72% or more) and the continuous stretches of T bases are on both ends of the ssDNA, these templates behaved as if they were homogeneous. Fig. 5*B* shows the normalized equilibrium titrations of CspB with T18C7T18, T14C7T14, T9C7T9, T7C7T7, and T5C7T5. It is clear that the $[ssDNA]_{0.5}$ for these ssDNA templates increases as the length of the ssDNA decreases, being more dramatic for T5C7T5. A similar effect was observed by Kowalczykowski *et al.* (20). They studied the binding of gene 32 protein to poly(rA) as a function of the oligonucleotide length (>400, 120, and 56 nucleotides). A rigorous binding analysis of the titration profiles showed that the affinity and cooperativity was the same for all three oligonucleotides, although more protein was needed to saturate the 56-mer poly(rA) than to saturate the 120-mer or >400 mer. This effect has been also observed for other proteins interacting with shorter oligonucleotides, *i.e.* the mitochondrial Y-box protein RBP16 interacting with guide RNAs. RBP16 has a cold shock domain and interacts with guide RNAs through an oligo(U) tail (21). This interaction required higher $[RNA]_{0.5}$ (defined as the molar excess required to achieve 50% inhibition of the RBP16 binding to ^{32}P-labeled guide RNA gA6) as the length of the oligo(U) decreased from 40 to 4 nucleotides (22).

Importance of the Relative Position of the T Bases in 23-mer ssDNA Templates—The effect of relative position of the T bases within ssDNA template was investigated by comparing the CspB binding to the 23GpTi series (the T bases are in the middle) and the 23pTiG series (in which the T bases are on both ends; see Table I for sequence) keeping constant the total length of the ssDNA template at 23 bases. Fig. 6 shows the normalized profiles for the titrations of CspB with the 23pTiG oligonucleotides. The binding curves for the 23pT20G, 23pT18G, and 23pT16G overlap. The CspB binding competence for these ssDNA templates is about 5.8×10^{-8} M, which is very close to the CspB binding competence for 23pT, 6.1×10^{-8} M (8). This result again indicates that when the T content in non-homogeneous ssDNA templates is high (70% in 23pT16G or more) and the T bases are on both ends of the ssDNA templates they behave as if they were homogeneous. We can also conclude, from this and previous results with the TiC7Ti series, that as long as the stretch in the middle is short enough (30% or less of the total length of the template) the oligonucleotide will behave as homogeneous 23pT independent of which bases are in the middle, C or G (Figs. 5*B* and 6*A*, respectively). As the T content in the ssDNA templates decreases (*e.g.* 23pT12G, 23pT8G, and 23pT6G series), there is a corresponding increase in the $[ssDNA]_{0.5}$ (Fig. 6*A*). To understand whether this effect is due to the difference in the number of T bases or due to the different position of these bases within the oligonucleotides, we plotted the $[ssDNA]_{0.5}$ for the 23pTiG and 23GpTi series as a function of the T content (percentage of T bases) in the ssDNA (Fig. 6*B*). The dependence of the CspB binding competences on the T content in the 23pTiG and 23GpTi templates is very comparable for both series of ssDNA, except for the 23pT6G template in which "end effects" or possible aggregation of the G bases may play a role. This similar behavior suggests that it is the T content in the ssDNA templates, and not its relative position, which defines the properties of CspB binding to T-based ssDNA, although some "end effects" cannot be completely ruled out. The importance of the "end effects" was clearly demonstrated for the interaction of the Y-box protein RBP16 from *Trypanosoma brucei*, which contains a cold shock domain motif, with 34-mer oligonucleotides (22). The 34-mer oligonucleotides had a patch of four adjacent uridylates, forming the binding site, and the rest of the oligonucleotide was oligo(dC). The tetraU patch was moved from 5′ to 3′ at certain intervals and the binding of RPB16 to these different templates was compared. It was shown that binding is weaker when tetraU patch was located close to the 5′ or 3′ ends of the template. Furthermore, Pelletier *et al.* (22) showed that the affinity also depends on whether tetraU patch is located at 5′ or 3′ end.

Effect of High Ionic Strength on the CspB Binding to Non-homogeneous ssDNA—It has been shown that CspB binding to 23pC is strongly dependent on the salt concentration and could be practically abolished in 1 M NaCl, whereas the CspB binding to 23pT is independent of salt concentration (8). These results were interpreted to mean that there are two different modes of CspB interactions with polypyrimidine ssDNA templates. In mode I, the interactions of CspB with poly(dC) occurs predom-

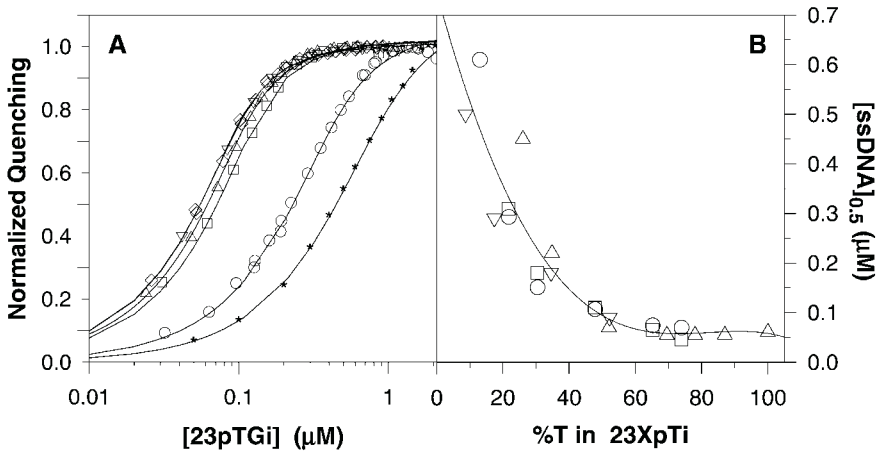

FIG. 6. *Panel A*, normalized quenching of the CspB Trp fluorescence intensity as a function of 23pT20G (◇), 23pT18G (▽), 23pT16G (△), 23pT12G (□), 23pT8G (○), and 23pT6G (*). Experimental conditions are as described in Fig. 1. *Panel B*, dependence of the $[ssDNA]_{0.5}$ on the T content of the oligonucleotide for 23pTiG (○), 23GpTi (□), and 23CpTi (△) series.

inantly through the phosphate backbone and thus is largely electrostatic and strongly dependent on the ionic strength. In mode II, the interactions of CspB with poly(dT) occurs predominantly through van der Waals and stacking interactions with the bases and are thus independent of the ionic strength. We thus investigated which of these two modes of interactions was involved in the CspB binding to non-homogeneous ssDNA templates. This was done by comparing the CspB binding to different oligonucleotides (with continuous and non-continuous stretches of T bases) measured in low (0.1 M) and high (1 M) NaCl concentrations. It was anticipated that if the CspB binding to C bases is independent of the presence of T bases, then under 1 M NaCl concentration the CspB binding to the C bases in the ssDNA would be dramatically impaired, which would translate in a lower quenching effect on the CspB Trp fluorescence upon binding. Qualitative results of the analyses presented in Table I show that the presence of 1 M NaCl did not affect the titration profiles of CspB with 23CpTi (i = 3–23 forming a continuous stretch of T bases). These results suggest that CspB interacts directly with the T bases, mainly through hydrogen bonding, van der Waals interactions, and hydrophobic effects, but not through electrostatic interactions of protein groups with the phosphate backbone. How many T bases are required in order to have a salt-independent binding? To answer this question, the interactions of CspB with two other ssDNA, 23CpT1 and 23CpT2, with just one or two T bases (Table I) at low and high salt concentrations were studied. It was found that for these two oligonucleotides there is an effect of 1 M NaCl on the titration profiles. The decrease, however, is not as pronounced as in the case of 23pC, where 1 M NaCl completely abolishes CspB binding (8). We thus can conclude that the switch from mode I to mode II of CspB-ssDNA interactions requires presence of at least 3 T bases in the template.

The only other templates, which also exhibit the dependence of the binding on the ionic strength, are $23CT_2$ and 23pT6G (Table I). In the case of $23CT_2$, such a behavior is understandable because this template contains only two T bases. The 23pT6G template contains six T bases arranged into two triplets. According to the observations made on the other ssDNA templates, the presence of three T bases should render salt-independent quenching effect on CspB-ssDNA interactions. However, these T bases are located at the 5′ and 3′ ends of the 23pT6G template, and the end effects might be important. Indeed, the effect on 1 M NaCl on CspB titration is significantly reduced in 23pT8G and completely abolished in 23pT12G (Table I). We thus propose that the switch from mode I to mode II binding for CspB ssDNA requires at least 3 T bases located *within* the ssDNA template or 4 T bases if located at the 5′ or 3′ ends.

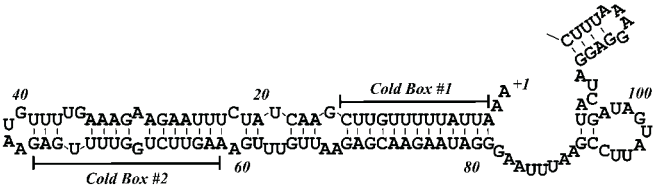

FIG. 7. **Possible secondary structure formation in the 5′-UTR of *cspB*.** The secondary structure was generated using RNAFold software based on the algorithm described by Zuker *et al.* (34). Cold shock boxes identified previously by Graumann *et al.* (7) are *underlined*.

These results suggest that the mechanism of the CspB interaction with most of the studied non-homogeneous T-based ssDNA templates is through the bases and does not involve electrostatic interactions of protein groups with the phosphate backbone. The large enthalpies of binding to the non-homogeneous T-based ssDNA templates (−105 ± 9 kJ/mol) also support this conclusion because binding to the 23pC (which is strongly salt-dependent) is accompanied by 4 times lower enthalpy, −25 ± 2 kJ/mol (8). Moreover, in terms of the binding enthalpy, the non-homogeneous T-based oligonucleotides behaved as the homogeneous 23pT, indicating that hydrogen bonding, van der Waals interactions, and hydrophobic effects are the major forces responsible for CspB binding to ssDNA templates (8).

DISCUSSION

In this study it has been shown that the ability of the cold shock protein CspB from *B. subtilis* to bind ssDNA templates correlates with the content of T bases present in the template. Moreover, the binding competences of CspB for continuous stretches of T are independent of the surrounding bases (Fig. 2), suggesting that the local structure of the ssDNA does not play significant role in the interactions. Comparable binding properties are observed when CspB binds continuous or non-continuous stretches enriched in T bases (Figs. 4, 5, and Fig. 6*B*). This result suggests that the presence of T is not equally important at all position of the binding site consisting of 6–7 bases. Our findings also strongly suggest that, in the CspB interaction with non-homogeneous ssDNA templates, it is the protein binding to the T bases which drives the interaction. Just three T bases are enough to switch the mechanism of interaction from CspB interacting with ssDNA phosphate backbone (like in 23pC) to CspB interacting directly with the bases (like in 23pT and most of the other studied ssDNA series) as the CspB binding becomes independent of the ionic strength (Table I). Our recent studies have shown that binding of CspB to ssDNA-template based on another pyrimidine nucleotide U is much more similar to the binding characteristics of 23pT

than 23pC (13). In particular, binding of CspB to 23pU under the conditions of high and low ionic strengths are comparable (13).

If the biological function of CspB is indeed related to its high affinity for stretches of ssDNA enriched in T bases, there are two T-rich regions identified in DNA. One occurs at factor-independent transcription termination signals (see Refs. 23–27 for reviews). The other is frequently located downstream from the promoter sequences, as part of the sequences contained within 5′-UTR of cold shock proteins (9). Recently, we have shown that the CspB binding parameters for 23pU are quite comparable to the ones for 23pT (13) (although the former has somewhat lower affinity, it might be related to the fact that we used d(pU) instead of r(pU)). There are two cold shock boxes enriched in U bases within the *cspB* 5′-UTR (Fig. 7), which are highly conserved in another member of the cold shock family of proteins from *B. subtilis*, the *cspC* 5′-UTR (7). We have performed CspB binding studies with each of these motifs using ssDNA templates with U bases substituted by T and found that CspB binds with high affinity, as it is expected from their high T content.[2] Thus, our results support the idea that indeed these motifs could have a regulatory role *in vivo* as suggested by Graumann *et al.* (7). Since the CspB binding affinity increases as the temperature decreases (8), the protein binding to the cold shock Box1 and Box2 is more favored at low temperatures. Protein binding to such regions would prevent formation of secondary structure of the 5′-UTR (Fig. 7); hence, CspB would facilitate translation at low temperatures. This 5′-UTR region has been shown to be important in stabilizing the mRNA for the major cold shock protein CspA from *E. coli* (28). Comparison of the 5′-UTRs among the cold shock proteins in *E. coli* clearly shows that the proteins that are cold-inducible (CspA, CspB, CspG, and CspI) have very long 5′-UTR (>100 bases) and have tendency to form similar secondary structures at low temperatures (Fig. 7). The same appears to be true for 5′-UTR of CspB and CspC from *B. subtilis*. The average Gibbs energy of secondary structure formation for the cold shock-inducible 5′-UTR calculated according to SantaLucia (29) is $-(260 \pm 50)$ kJ/mol. However, those proteins that are not cold-inducible (CspC, CspD, CspE) have short 5′-UTRs (40–90 bases), have relatively low secondary structure stability, $-(120 \pm 50)$ kJ/mol, and thus low tendency to fold at low temperatures. This correlation suggests that, upon cold shock, the increase in CspB induction might be essential for keeping its 5′-UTR region unstructured. Comparison of the 5′-UTR regions among cold shock proteins in *E. coli* has showed that there is a well conserved 11-base sequence (cold shock box) (28). However, the sequence of the cold shock box in the 5′-UTR of cold-inducible proteins in *E. coli* (UGACGUACAGA) is very different from the cold shock boxes found in the same region in *B. subtilis* (AUUAUUUUUGUUC) that is very rich in U bases (Fig. 7). It is conceivable that cold shock proteins have diverse functions. The ability to facilitate transcription antitermination has been suggested for CspA from *E. coli* (30), whereas *B. subtilis* CspB might be preventing mRNA folding and thus facilitating translation at low temperatures. This possible functional difference is supported by the observation that cold-inducible proteins from different bacteria may recognize different sequences, as we have already demonstrated for CspB from *B. subtilis* and CspA from *E. coli* (8, 13).

Our results suggest a model for the role of the cold shock protein CspB from *B. subtilis*. At low temperatures and low concentration of CspB, the nascent mRNA will fold, thus interfering with translation. It is important to note that cold shock boxes are located within two putative stem structures of the 5′-UTR (Fig. 7). In the presence of CspB, protein binding to the cold shock boxes 1 and 2 can be the driving force to prevent the mRNA to adopt stem structure. Thus, CspB binding will effectively prevent secondary structure formation and thus will facilitate translation. Probably, two CspB molecules will bind with high affinity per each of two cold shock boxes, as these boxes are about 14 nucleotides long and, although not completely homogeneous, are highly enriched in U bases (Fig. 7). This would suggest that cold shock proteins possess RNA-chaperone activity (31), a possible function of cold shock proteins that is in accord with the earlier observations. It has been shown that both CspA (32, 33) and CspB (7) bind RNA and increase its susceptibility to the ribonuclease digestion, thus indicating that CspA/CspB binding prevents the formation of secondary structure of RNA, *i.e.* acting as an RNA chaperone.

Acknowledgments—We thank Dr. Michael Fried for many helpful suggestions and Miyo Sakai for performing experiments on Beckman XL-A.

[2] M. M. Lopez and G. I. Makhatadze, unpublished results.

REFERENCES

1. Inouye, M. (1999) *J. Mol. Microbiol. Biotechnol.* **1,** 191
2. Yamanaka, K. (1999) *J. Mol. Microbiol. Biotechnol.* **1,** 193–202
3. Graumann, P. L., and Marahiel, M. A. (1999) *J. Mol. Microbiol. Biotechnol.* **1,** 203–209
4. Willimsky, G., Bang, H., Fischer, G., and Marahiel, M. A. (1992) *J. Bacteriol.* **174,** 6326–6335
5. Schindelin, H., Marahiel, M. A., and Heinemann, U. (1993) *Nature* **364,** 164–168
6. Schnuchel, A., Wiltscheck, R., Czisch, M., Herrler, M., Willimsky, G., Graumann, P., Marahiel, M. A., and Holak, T. A. (1993) *Nature* **364,** 169–171
7. Graumann, P., Wendrich, T. M., Weber, M. H., Schroder, K., and Marahiel, M. A. (1997) *Mol. Microbiol.* **25,** 741–756
8. Lopez, M. M., Yutani, K., and Makhatadze, G. I. (1999) *J. Biol. Chem.* **274,** 33601–33608
9. Schroder, K., Graumann, P., Schnuchel, A., Holak, T. A., and Marahiel, M. A. (1995) *Mol. Microbiol.* **16,** 699–708
10. Epstein, I. R. (1978) *Biophys. Chem.* **8,** 327–339
11. Makhatadze, G. I., and Marahiel, M. A. (1994) *Protein Sci.* **3,** 2144–2147
12. Wallace, R. B., and Miyada, C. G. (1987) *Methods Enzymol.* **152,** 432–442
13. Lopez, M. M., and Makhatadze, G. I. (2000) *Biochim. Biophys. Acta* **1479,** 196–202
14. Lohman, T. M., and Bujalowski, W. (1991) *Methods Enzymol.* **208,** 258–290
15. Lohman, T. M., and Mascotti, D. P. (1992) *Methods Enzymol.* **212,** 424–458
16. Lohman, T. M., and Mascotti, D. (1992) *Methods Enzymol.* **212,** 400–424
17. McGhee, J. D., and von Hippel, P. H. (1974) *J. Mol. Biol.* **86,** 469–489
18. Ferrari, M. E., Bujalowski, W., and Lohman, T. M. (1994) *J. Mol. Biol.* **236,** 106–123
19. Graumann, P., and Marahiel, M. A. (1994) *FEBS Lett.* **338,** 157–160
20. Kowalczykowski, S. C., Paul, L. S., Lonberg, N., Newport, J. W., McSwiggen, J. A., and von Hippel, P. H. (1986) *Biochemistry* **25,** 1226–1240
21. Hayman, M. L., and Read, L. K. (1999) *J. Biol. Chem.* **274,** 12067–12074
22. Pelletier, M., Miller, M. M., and Read, L. K. (2000) *Nucleic Acids Res.* **28,** 1266–1275
23. Adhya, S., and Gottesman, M. (1978) *Annu. Rev. Biochem.* **47,** 967–996
24. Rosenberg, M., and Court, D. (1979) *Annu. Rev. Genet.* **13,** 319–353
25. Platt, T. (1986) *Annu. Rev. Biochem.* **55,** 339–372
26. Richardson, J. P. (1993) *Crit. Rev. Biochem. Mol. Biol.* **28,** 1–30
27. Henkin, T. M. (1996) *Annu. Rev. Genet.* **30,** 35–57
28. Jiang, W., Fang, L., and Inouye, M. (1996) *J. Bacteriol.* **178,** 4919–4925
29. SantaLucia, J. J. (1998) *Proc. Natl. Acad. Sci. U. S. A.* **95,** 1460–1465
30. Bae, W., Xia, B., Inouye, M., and Severinov, K. (2000) *Proc. Natl. Acad. Sci. U. S. A.* **97,** 7784–7789
31. Herschlag, D. (1995) *J. Biol. Chem.* **270,** 20871–20874
32. Jiang, W., Hou, Y., and Inouye, M. (1997) *J. Biol. Chem.* **272,** 196–202
33. Phadtare, S., and Inouye, M. (1999) *Mol. Microbiol.* **33,** 1004–1014
34. Zuker, M., and Stiegler, P. (1981) *Nucleic Acids Res.* **9,** 133–148